



HAL
open science

Differential microstructural development within sensorimotor cortical regions: A diffusion MRI study in preterm and full-term infants

Alexandra Brandstaetter, Andrea Gondová, Laurie Devisscher, Denis Rivière, Guillaume Auzias, Yann Leprince, Jessica Dubois

► **To cite this version:**

Alexandra Brandstaetter, Andrea Gondová, Laurie Devisscher, Denis Rivière, Guillaume Auzias, et al.. Differential microstructural development within sensorimotor cortical regions: A diffusion MRI study in preterm and full-term infants. *Developmental Cognitive Neuroscience*, 2025, 75, pp.101610. <10.1016/j.dcn.2025.101610>. <hal-05347574>

HAL Id: hal-05347574

<https://amu.hal.science/hal-05347574v1>

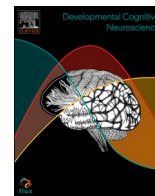
Submitted on 4 Nov 2025

HAL is a multi-disciplinary open access archive for the deposit and dissemination of scientific research documents, whether they are published or not. The documents may come from teaching and research institutions in France or abroad, or from public or private research centers.

L'archive ouverte pluridisciplinaire HAL, est destinée au dépôt et à la diffusion de documents scientifiques de niveau recherche, publiés ou non, émanant des établissements d'enseignement et de recherche français ou étrangers, des laboratoires publics ou privés.



Distributed under a Creative Commons CC BY 4.0 - Attribution - International License



Differential microstructural development within sensorimotor cortical regions: A diffusion MRI study in preterm and full-term infants

Alexandra Brandstaetter^{a,b}, Andrea Gondová^{a,b,c,d,*}, Laurie Devisscher^{a,b}, Denis Rivière^e, Guillaume Auzias^f, Yann Leprince^b, Jessica Dubois^{a,b}

^a Université Paris Cité, Inserm, NeuroDiderot, Paris F-75019, France

^b Université Paris-Saclay, CEA, NeuroSpin, UNIACT, Gif-sur-Yvette F-91191, France

^c Fetal Neonatal Neuroimaging and Developmental Science Center, Boston Children's Hospital, Harvard Medical School, Boston, MA, USA

^d Division of Newborn Medicine, Boston Children's Hospital, Harvard Medical School, Boston, MA, USA

^e Université Paris-Saclay, CEA, CNRS, Neurospin, BAQBAB, Gif-sur-Yvette 91191, France

^f Aix Marseille University, CNRS, Inst Neurosci Timone, UMR7289, Marseille 13005, France

ARTICLE INFO

Keywords:

Pre-central and post-central gyrus
Somatotopic maps
Maturation
Prematurity
Vulnerability

ABSTRACT

The sensorimotor system develops early in utero and supports the emergence of body representations critical for perception, action, and interaction with environment. While somatotopic protomaps are already developed in the primary somatosensory and motor cortices in late pregnancy, little is known about the anatomical substrates of this functional specialization. In this study, we aimed to decipher the microstructural properties of these regions in the developing brain. Using advanced diffusion MRI and post-processing tools, we parcellated the pre- and post-central gyri into microstructurally distinct clusters along the lateral-to-medial axis in 25 full-term neonates, confirming the early differentiation within sensorimotor regions. These clusters were further analyzed in 59 preterm infants scanned at term-equivalent age (TEA, PT_{TEA}), of which 45 were also scanned near birth (PT_{Birth}), and compared with another group of 59 full-term neonates. Applying a multivariate Mahalanobis distance approach, we quantified deviations in preterm cortical microstructure relative to the full-term reference. Preterm infants showed significant region- and position-specific deviations at both ages, though these were smaller at TEA (repeated-measures ANCOVA: PT_{Birth} : region effect $F=25.48$, position effect $F=16.06$; PT_{TEA} : region effect $F=14.87$, all $p < 0.001$), consistently with ongoing maturation during the pre-term period. Differences between the pre- and post-central gyri, and along the somatotopic axis, suggested differential vulnerability to prematurity. In particular, compared with somatosensory regions, the motor regions appeared to be at a more advanced stage of maturation close to birth (paired t-test, $T = -4.388$, $p < 0.001$) and less vulnerable at TEA (paired t-test, $T = -4.169$, $p < 0.001$), suggesting lesser impact of prematurity. An opposite pattern was observed, particularly close to birth, for lateral positions related to mouth representation compared with intermediary (paired t-test: $T = 5.933$, $p < 0.001$) and medial (paired t-test: $T = 4.712$, $p < 0.001$) positions. These findings support the notion that early sensorimotor cortical specialization is microstructurally emergent during gestation and sensitive to atypical developmental context of preterm birth.

1. Introduction

The sensorimotor system is one of the first to develop *in utero* in interaction with other sensory functions to facilitate the perception, integration and emotional processing of environmental information. In addition to early genetic and epigenetic factors, this early development is thought to depend on the multiple somatosensory stimulations and motor experiences of the foetus and then the baby (e.g., tactile contacts

through the continuous pressure of the amniotic fluid over the body and with the mother's uterine membrane, feedback from spontaneous motor behaviours) (de Vries et al., 1982; Fagard et al., 2018). At the neural level, the early establishment of thalamocortical afferent connections to the subplate (Kostović et al., 2019) is supposed to provide the basis for the cortical processing of such sensorimotor activity from mid-gestation. Underlying cortical regions seem to be partly specialized at an early stage, as suggested by functional MRI (fMRI) studies of preterm and

* Corresponding author at: Université Paris Cité, Inserm, NeuroDiderot, Paris F-75019, France.

E-mail addresses: Gondova.Andrea@outlook.com, andrea.gondova@childrens.harvard.edu (A. Gondová).

<https://doi.org/10.1016/j.dcn.2025.101610>

Received 10 June 2025; Received in revised form 4 August 2025; Accepted 27 August 2025

Available online 30 August 2025

1878-9293/© 2025 The Authors. Published by Elsevier Ltd. This is an open access article under the CC BY license (<http://creativecommons.org/licenses/by/4.0/>).

full-term neonates showing localized responses to tactile and passive motor stimulations (e.g., Allievi et al., 2016; Dall'Orso et al., 2018; Eyre et al., 2021). In particular, a proto somatotopy has been described during an equivalent period to the third trimester of gestation (Dall'Orso et al., 2018), with a topographic representation of body parts in the pre-central and post-central gyri (considered as primary somatosensory and motor cortices, respectively), from tongue to toes along the lateral-ventral to medial-dorsal axis of the classical 'homunculus' model reported in adults by (Penfield and Boldrey, 1937). A certain spatial organization of functional connections between these regions also seems to be present early on, leading to an adult-like configuration by the time of full-term birth (Dall'Orso et al., 2022). Such complex functional organization is assumed to be fundamental for motor skill acquisitions, imitation and social interactions during infancy (Marshall and Meltzoff, 2015).

Nevertheless, early neurodevelopmental disturbances and alterations in environmental influences might impact such cerebral organization, with possible long-term consequences on the child behavioral acquisitions and learnings. A common example is preterm birth (i. e., delivery before 37 weeks of gestational age - w GA – which affects over 10 % of newborns every year) (Martin et al., 2023). Preterm neonates experience strong changes in physiological and physical conditions (e.g., reduced movements due to gravity outside the womb) (Anderson, 1986; Fyfe et al., 2014; Teune et al., 2011), as well as early *ex utero* exposure to the environment of the neonatal intensive care unit (e.g., possible aggressive sounds, lights, limited tactile contacts), and painful medical procedures (Cong et al., 2017; Flacking et al., 2012). According to the embodied brain model, such exposure due to prematurity might impair the development of somatotopic organization (Yamada et al., 2016), though direct *in vivo* evidence is lacking.

Besides, a number of studies in preterm infants have shown developmental disturbances of the brain sensorimotor system, even in the absence of overt brain lesions, using advanced anatomical and diffusion MRI (dMRI) approaches (Dubois et al., 2021; Ouyang et al., 2019a). Notably, complex microstructural models (e.g., neurite orientation dispersion and density imaging NODDI) have appeared informative to analyse multi-shell dMRI data compared to the diffusion tensor imaging (DTI), and multiparametric methods may help integrating complementary measures. For example, our previous work demonstrated that white matter connections within the sensorimotor network are differentially impacted by prematurity at term equivalent age, with a caudal-to-rostral vulnerability that might mirror the typical progression of maturation (Neumane et al., 2022).

Additionally, prematurity impacts the microstructural maturation of cortical regions across the whole brain (e.g. (Ball et al., 2013; Batalle et al., 2019; Gondová et al., 2025; Ouyang et al., 2019). Of note, over this early developmental period, advanced maturation of cortical grey matter is generally associated with a decrease in DTI-derived fractional anisotropy (FA), as well as axial, radial and mean diffusivities (AD, RD, MD) and an increase in NODDI-derived orientation dispersion index (ODI), which might reflect the decrease in the early highly radial organization of the cortex whose microstructural complexity progressively increases with maturation and neurite growth. Besides the developmental pattern of neurite density index (NDI) that quantifies intra-neurite space within tissues is plausibly more complex (with a pre-term decrease followed by an increase), reflecting the growth of dendritic arborization and neurites, the increasing cellular and organelle density contrasting with cortical expansion (Batalle et al., 2019). In addition to cortical characteristics, prematurity seems to modulate the covariation of microstructural properties between cortical regions (named "microstructural connections") differently in the sensorimotor network compared to the visual and associative networks (Gondová et al., 2025).

This underscores the importance of evaluating whether prematurity impacts the somatotopic organization of sensorimotor regions. While we might expect a global impact on the progression of specialization, we

also hypothesize differential effects depending on which body parts become progressively functional and used. However, systematic mapping with fMRI in neonates remains challenging. As an alternative first step, we propose evaluating the microstructural properties of these cortical regions. Recent studies in adults have suggested strong links between body representations within the pre- and post-central gyri, the morphological patterns of the central sulcus separating them (Germann et al., 2020), and their myeloarchitecture (Kuehn et al., 2017). Furthermore, in a study comparing full-term neonates to adults, we showed that anatomically defined parcels of these gyri show distinct microstructural properties and a different progression of maturation over the perinatal weeks (Chauvel et al., 2020; Devisscher et al., 2021).

In this study, we then aimed to delineate regions within pre- and post-central gyri based on local microstructural properties at full-term birth and assess whether the resulting parcels are differentially affected by prematurity and whether they show different maturational patterns during a period equivalent to the last trimester of gestation. We used an advanced dMRI multi-parametric approach to compare preterm infants scanned close to birth and at term equivalent age with full-term neonates. We hypothesized that a data-driven method would allow us to reveal distinct cortical clusters within pre- and post-central gyri, which would have a somatotopic significance as suggested by mapping studies in adults. We further assumed that 1) sensory vs motor clusters, and 2) lateral vs medial clusters (related to different body parts) would show a different vulnerability to prematurity as well as a different developmental progression in the pre-term period, reflecting the fact that different sensorimotor functions emerge at different times and with different rhythms during early development.

2. Methods

2.1. Data presentation

2.1.1. Subjects

This study included a sample of preterm and full-term neonates from the 3rd release of the developing Human Connectome Project (dHCP) database (Edwards et al., 2022), collected at St Thomas' Hospital, London, UK, between 2015 and 2020. The project received approval from the UK NHS Research Ethics Committee (14/LO/1169, IRAS 138070), and written informed consent was obtained from the parents of all participants.

Our analysis focused on four subject groups: PT_{TEA} consisting of 59 low-risk preterm-born infants scanned at term-equivalent age (TEA) (33 males and 26 females, median gestational age (GA) 31.7 weeks (w) [23.7–36.0w]; median postmenstrual-age (PMA) at MRI 41.3w [38.4–44.9w]); PT_{Birth} consisting of 45 subjects from the PT_{TEA} group that were scanned close to birth (26 males and 19 females, median GA at birth 32.3w [25.6–36.0w]; median PMA at MRI 34.9w [28.3–36.9w]). As a normative reference, we used a group of 59 full-term (FT) neonates matched to PT_{TEA} infants according to PMA at MRI and sex (FT_{Ref}: median GA at birth 40.1w [37.4–42.3w]; median PMA at MRI 41.3w [38.3–44.3w]; mean PMA difference between PT_{TEA} and FT_{Ref} matched subjects: 0.02w). Although we did not match on other factors such as radiology scores, all selected subjects were without atypical neuro-imaging findings.

Additionally, an independent group of 25 FT infants (FT_{Ind}: median GA at birth 40.1w [37.1–41.4w]; median PMA at MRI 41.3w [38.1–43.9w]), with similar subject characteristics to FT_{Ref} in terms of PMA at MRI, GA at birth and sex distribution, was used for defining the cluster-based cortical parcellation. Subject characteristics are detailed in Table 1. See Supplementary Fig. 1 for distribution of ages for the four cohorts.

2.1.2. Acquisition and preprocessing of MRI data

MRI data were acquired using a Philips 3 Tesla Achieva scanner (Philips Medical Systems, Best, Netherlands). All infants were scanned

Table 1

Group characteristics. *Legend:* FT_{Ind}: independent full-term group, FT_{Ref}: reference full-term group, GA: gestational age, N: number, PMA: post-menstrual age, PT_{Birth}: preterm group scanned close to birth, PT_{TEA}: preterm group scanned at term equivalent age (TEA).

	PT _{Birth}	PT _{TEA}	FT _{Ref}	FT _{Ind}
N	45	59	59	25
Sex:				
males	26	33	33	15
females	19	26	26	10
Median GA at Birth	32.3 [25.6	31.7	40.1 [37.1	40.1 [37.1
[range] in weeks	- 36.0]	[23.7-36.0]	- 42.3]	- 41.1]
Median PMA at Scan	34.9 [28.3	41.3 [38.4 -	41.3 [38.3	41.3 [38.3
[range] in weeks	- 36.9]	44.9]	- 44.3]	- 43.9]

during natural sleep using a neonatal head coil and imaging system optimized for the dHCP study as previously described (Hughes et al., 2017). Here, we considered anatomical and diffusion MRI data available in its pre-processed state (Edwards et al., 2022).

The *anatomical data* resulted from acquisition and reconstruction of T2w images using optimized protocols (Cordero-Grande et al., 2019), leading to super-resolved images with an isotropic spatial voxel size of 0.5 mm. Processing followed a dedicated pipeline for brain tissue segmentation and cortical surface extraction of neonatal brains (Makropoulos et al., 2018), with bias-correction, brain extraction, volumetric segmentation using Draw-EM (Developing brain Region Annotation With Expectation Maximization) algorithm (Makropoulos et al., 2014). Interface between cortex and white matter (*wm surfaces*) were then extracted following an adapted pipeline with Morphologist toolbox (BrainVISA 5.1.1) (Rivière et al., 2009).

Diffusion MRI data (dMRI) were acquired following a multi-shell high angular resolution diffusion imaging (HARDI) protocol with 4 b-shells ($b = 0$ s/mm²: 20 repeats; and $b = 400, 1000, 2600$ s/mm²: 64, 88, and 128 directions, respectively) (Hutter et al., 2018) and pre-processed with *SHARD pipeline*, which includes denoising, Gibbs ringing correction, fat shift suppression, susceptibility distortion correction, and motion correction with slice-to-volume reconstruction using the SHARD method (Christiaens et al., 2021), leading to an isotropic voxel size of 1.5 mm. Data quality across the subject groups is visualised in [Supplementary Figure 2](#).

2.2. Diffusion modelling and metric extraction

For each subject, the DTI model was fitted to the diffusion data using a single shell ($b = 1000$ s/mm²) and calculated with FSL's DTIFIT to estimate metric maps for 4 metrics: axial diffusivity (AD), radial diffusivity (RD), and mean diffusivity (MD), fractional anisotropy (FA). Additionally, multi-shell diffusion data was used to derive the neurite density index (NDI) and orientation dispersion index (ODI) maps from the NODDI model (Zhang et al., 2012) using the CUDA 9.1 Diffusion Modelling Toolbox (cuDIMOT) NODDI Watson model implementation for GPUs (Hernandez-Fernandez et al., 2019). Derived NODDI maps were then corrected as described in (Neumane et al., 2022). Diffusion metrics were then computed within the cortical ribbon using an optimized methodology limiting the partial volume effects from adjacent white matter and cerebrospinal fluid: this involved the projection of values to the *wm surface* using a cylindrical approach guided by the minimum of AD, as described in (Gondová et al., 2023; Lebenberg et al., 2019).

2.3. Microstructure-based clustering of pre- and post-central gyri

To derive microstructure-based clusters of the pre- and post-central cortical gyri distributed along the latero-medial axis in order to investigate their putative correspondence with somatotopic mapping, we opted for an approach combining initial manual delineation of region

subdivisions with agglomerative clustering to refine and reduce cluster numbers. We first selected a single subject from the FT_{Ind} group and the two gyri were delineated bilaterally using the M-CRIB-S surface-based parcellation tool optimized for term-born neonates (Adamson et al., 2020). We then subdivided each of the four parcels (2 gyri x 2 hemispheres) into 11 subdivisions providing a sufficient degree of details and of roughly similar size. This was guided by *geometrical coordinates* along the central sulcus reconstructed using an adapted Sulcus Parameterization toolbox (Cykowski et al., 2008; Dornier et al., 2025), and *latitude/longitude coordinates* along the gyri computed with Hip-Hop Cortical Parameterization of the Cortical Surface (Auzias et al., 2013) (both toolboxes available in BrainVISA 5.1.1). To refine region definitions and reduce the number of regions, we aimed to further cluster the initial subdivisions based on their microstructural similarity, but considering a group of neonates was then required to avoid biasing the results by the choice of the initial subject. We thus projected the 11 subdivisions per region into the anatomical space of the remaining 24 FT_{Ind} subjects using non-linear transformations via the 40w dHCP template from the dHCP database that were computed using Multimodal Surface Matching (MSM) approach (Bozek et al., 2018). We then checked the quality of the projected delineations, manually refined them if necessary to ensure their spatial consistency and anatomical correspondence across the subjects. For each subdivision of each gyrus at the subject level, we extracted the median values of the 6 diffusion metrics at the subject level, then concatenated these across FT_{Ind} subjects and hemispheres (to ensure correspondence between hemispheres during clustering) resulting in a subdivision-specific vector of length 300 (25 subjects x 2 hemispheres x 6 metrics for each of the 11 subdivisions). We then applied agglomerative hierarchical clustering with average linkage and Euclidean distance independently for the pre- and post-central gyri. The final number of clusters was selected based on visual inspection of the dendrograms to balance two goals: cluster quality (as reflected in branch lengths measuring within-cluster variance under Ward's criterion) and a reasonable final number of regions (with comparable number of clusters across gyri, and clusters of comparable size within gyrus) for interpretability. As the dendrograms showed relatively clear separation, no additional cluster selection methods were used. These clusters were then projected to all infants of the PT_{Birth}, PT_{TEA}, and FT_{Ref} groups as described earlier. Cluster borders were manually refined, and DTI and NODDI metrics were extracted for each cluster and subject. Summary of the pipeline is visualised in [Fig. 1](#).

To assess the validity our microstructure-based clusters, we conducted Welch's t-tests for each median metric per cluster to ensure the two FT groups did not significantly differ in terms of microstructure within each cluster. Additionally, we performed a repeated-measure analysis of covariance (ANCOVA) across the PT_{TEA} and FT_{Ref} groups to provide a first evaluation of the effects of prematurity (group effect), and clusters (region effect: pre- vs post-central; position effect: lateral, intermediary vs medial) on raw diffusion metrics. For this analysis, we decided not to test the interaction between group and clusters as this question is the focus of further analyses with the multi-parametric approach. Covariates included (1) PMA at MRI, and (2) residual whole-cortex metrics corrected for PMA (i.e. residuals from a linear regression of the given diffusion metric's median values across *inner cortical surfaces* of the two hemispheres with PMA, with the group mean added back to retain scale) to account for inter-subject variability in cortical maturation. The hierarchical structure of the repeated measures (matched PT-FT subjects across the two regions and three positions) were accounted for using a nested error term. As post-hoc tests, we subsequently compared region differences in diffusion metrics (after concatenating region values across positions), and position differences (after concatenating position values across regions) within FT_{Ref} group, using paired t-tests. For all analyses, statistical implementations were performed using R (version 2022.07.1) and the Pingouin (v0.5.4) Python package. Throughout our work, multiple comparisons were corrected using the Benjamini-Hochberg False Discovery Rate (FDR)

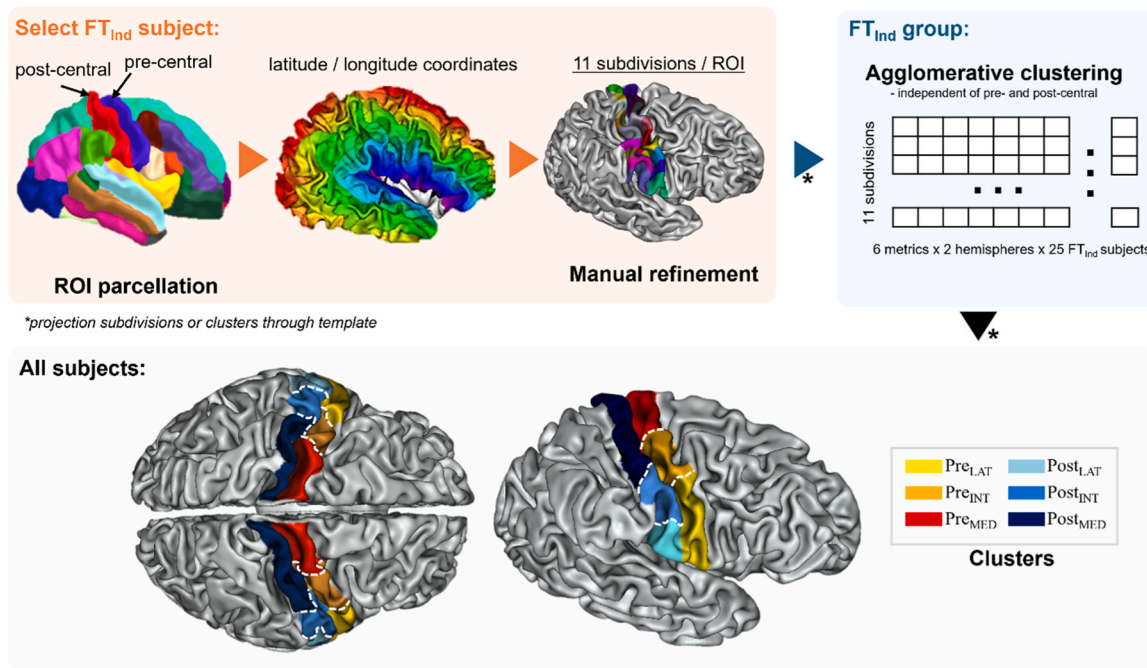


Fig. 1. Summary of the pipeline for microstructure-based clustering of pre- and post-central regions of interest (ROI) used in our work as well as visualization of the resulting clusters. *Legend:* Pre_{LAT} / Post_{LAT}: lateral portion of pre-central gyrus (yellow) / lateral portion of post-central gyrus (light blue), Pre_{INT} / Post_{INT}: intermediary portion of pre-central gyrus (orange) / intermediary portion of post-central gyrus (blue), Pre_{MED} / Post_{MED}: medial portion of pre-central gyrus (red) / medial portion of post-central gyrus (indigo).

method, with $\alpha = 0.05$ for all tests.

2.4. Multivariate analysis of prematurity and maturation effects within pre- and post-central gyri

To further characterise the impact of prematurity and maturation on the microstructural profiles of PT subjects compared to FT_{Ref} subjects for each cortical cluster, we applied a multivariate approach based on Mahalanobis distance accounting for the 6 diffusion metrics. This method measures the distance between an individual PT subject and the FT_{Ref} group as a reference, accounting for inter-subject variability within the FT_{Ref} group and the collinearity between diffusion metrics. This method measures the distance between an individual PT subject and the FT_{Ref} group as a reference, accounting for inter-subject variability within the FT_{Ref} group and the collinearity between diffusion metrics. A smaller distance indicates that the PT subject is closer to the reference group. This approach has previously been successfully used to study differential maturation across white matter tracts during infancy (Kulikova et al., 2015) and the effects of prematurity across sensorimotor tracts (Neumane et al., 2022).

To compute the Mahalanobis distances, we first calculated the median of each diffusion metric (AD, RD, MD, FA, NDI, ODI) for each cluster across the two hemispheres, scaled the values to a [0; 1] range across the clusters for each metric and group, and corrected them within each subject group for PMA at can, and for corresponding residual diffusion metrics over the whole cortex (corrected for PMA at scan, with the group mean added back to retain scale). Gestational age (GA) at birth was not included as a covariate, as it had minimal influence on individual metrics (data not shown) and was instead a variable of interest to evaluate whether GA influenced the prematurity distances (see below). Sex was also not controlled for due to limited sample size, although it may contribute to inter-individual variability.

We then computed the Mahalanobis distance in each cluster for both PT groups, using FT_{Ref} infants as the reference group representing typical variation of cluster brain microstructural characteristics at TEA. The Mahalanobis distance in PT_{TEA} infants (N = 59) would reflect the

cluster's deviation due to prematurity, while in PT_{Birth} infants (N = 45), the distance would indicate the level of immaturity during the preterm period. We assessed whether PT groups differed from FT_{Ref} group by testing the nullity of the Mahalanobis distance using t-tests for all clusters (corrected for 6 comparisons across clusters within each group). We also conducted additional ANCOVA analyses within each PT group to quantify the effects of different regions (pre/post-central) and positions (from lateral to medial) on the estimated Mahalanobis distance (including GA at birth as a covariate) and subsequently compared the observed differences between regions and between positions with paired t-tests. We then examined the relationship between the Mahalanobis distances in PT_{TEA} and the subjects' GA at birth using linear regression to assess whether the extent of prematurity impact on each cluster at TEA is associated with the level of prematurity at birth.

3. Results

3.1. Microstructure-based clusters of the pre- and post-central gyri

Visual inspection of dendrograms resulting from the clustering analysis of the 11 subdivisions across the 25 neonates of the FT_{Ind} group revealed clear clusters in both the pre-central and post-central gyri (Supplementary Figure 2). Three homotopic clusters were identified in each gyrus of the left and right hemispheres (Fig. 1), along the lateral-to-intermediary-to-medial position of both gyri: Pre_{LAT}, Pre_{INT}, Pre_{MED} for the pre-central gyrus, and Post_{LAT}, Post_{INT}, Post_{MED} for the post-central gyrus. By construction, these clusters showed distinct microstructural patterns in the FT_{Ind} group. But this was also the case in the other groups when clusters were projected to all infants (Fig. 2, see description below). As expected, the two FT groups did not show significant differences across the median diffusion metrics per cluster, as assessed using Welch's t-tests, except for ODI (Supplementary Table 1), suggesting similar microstructural characteristics and equivalent representation of normal brain development across computational steps in our study.

When the identified clusters were considered to characterize the

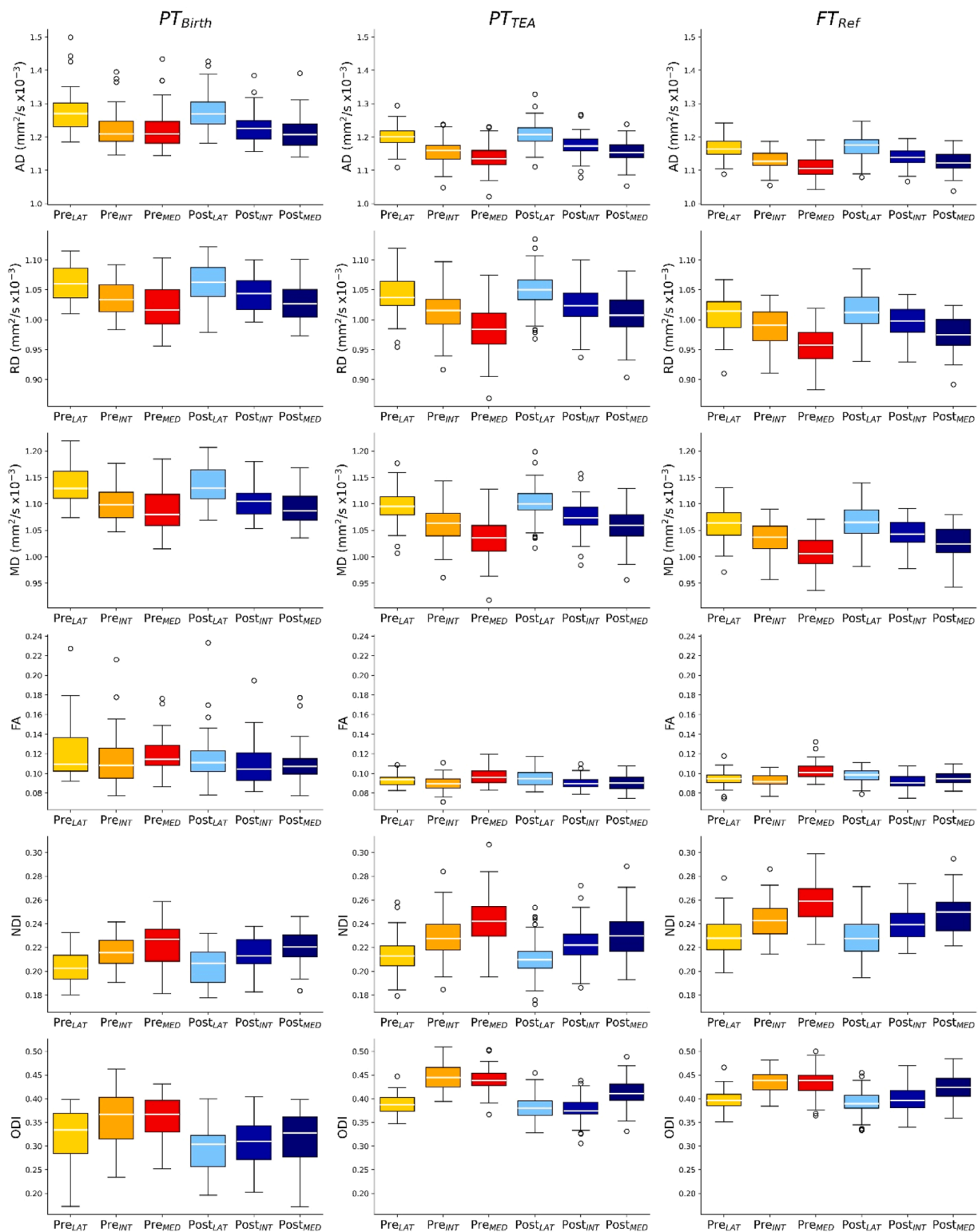


Fig. 2. Diffusion metrics across subject groups and pre- and post-central clusters. *Legend:* AD: axial diffusivity, RD: radial diffusivity, MD: mean diffusivity, FA: fractional anisotropy, NDI: neurite density index, ODI: orientation dispersion index. See Table 1 for subject group legend and Fig. 1 for cluster legend and colour-codes.

microstructural profiles of the groups of interest (PT_{Birth} , PT_{TEA} , and FT_{Ref}), we observed variations across pre-central and post-central regions, positions and groups (Fig. 2). Visual observations suggested a consistent spatial pattern along the lateral-to-medial axis in both gyri (e.g., higher diffusivity values in lateral than medial clusters). And as expected, systematic differences between the PT_{Birth} group compared to

the PT_{TEA} and FT_{Ref} groups were visible: higher diffusivity and FA values contrasting with lower NDI and ODI values in PT_{Birth} infants, although ODI showed considerable variability within this group.

Further comparisons of the PT_{TEA} and FT_{Ref} groups using ANCOVA modelling on each individual diffusion metric confirmed the influence of prematurity on microstructural characteristics (group effect for all

metrics), as well as significant effects of region and position (Supplementary Table 2a). Post-hoc paired t-tests within the FT_{Ref} group for the effect of region revealed consistently higher AD, RD, and MD, and lower FA, NDI, and ODI in the post-central compared to the pre-central gyrus (Supplementary Table 2b). Position-wise post-hoc tests showed significant differences across all metrics: AD, RD, and MD decreased from lateral to medial clusters, while NDI and ODI increased. FA followed a similar trend to NDI/ODI, except for higher values in the lateral vs. intermediate cluster (Supplementary Table 2c).

Taken together, these first results highlighted the importance of analysing clusters separately within each region and position, as they showed distinct effects on diffusion metrics, suggesting variations in underlying microstructural properties and potentially different impact of prematurity and maturation. Nevertheless, the variability across

individual metrics complicated the identification of clear patterns. A multivariate framework was thus needed to better capture and interpret prematurity effects and maturational differences across clusters, as outlined below.

3.2. Multivariate analysis of the impact of prematurity and maturation on microstructural profiles of pre- and post-central gyri

Mahalanobis distances for the 6 bilateral clusters for the two preterm groups are summarized in Fig. 3a, with lower values indicating that a subject's microstructural profile is more similar to the full-term reference (FT_{Ref}) distribution. By examining the Mahalanobis distances in the PT_{Birth} group, we can infer the degree of maturational changes within each cluster during the preterm period. In this group, all clusters showed

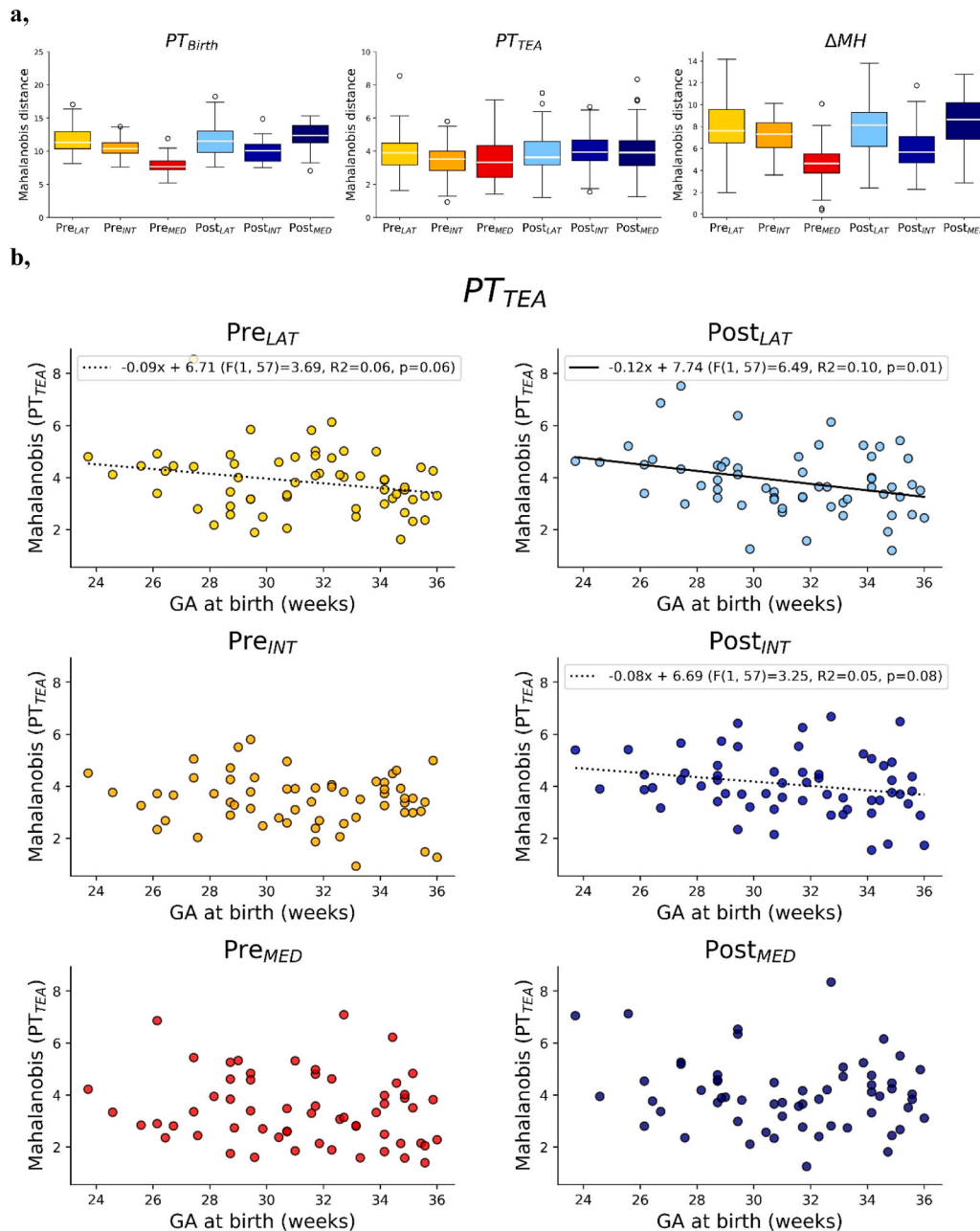


Fig. 3. a. Mahalanobis distances across clusters for PT_{Birth} (left), PT_{TEA} (middle) groups, as well as Mahalanobis distance differences between the two sessions for the subjects with longitudinal data. b. Scatter plots presenting relationship of Mahalanobis distance at TEA with GA at birth (solid line shows linear regressions association with $p < 0.05$ and dashed line with $p < 0.1$ after FDR correction across the 6 clusters). See Table 1 for subject group legend and Fig. 1 for cluster legend and colour-codes.

significant deviations from 0 (Supplementary Table 3), suggesting detectable ongoing maturational changes. The ANCOVA analysis over this group showed significant effects of both region (pre- and post-central gyri) and position, indicating heterogeneous microstructural maturation across the two gyri and the lateral to medial axis, but no effect of gestational age at birth. Pre_{MED} showed the smallest Mahalanobis distance, suggesting it might be the most developmentally advanced among the clusters close to birth. In contrast, Pre_{INT} and Pre_{LAT} displayed larger distances indicating they will undergo more pronounced maturational changes during the preterm period. A similar gradient somewhat appears to be present for the clusters in the post-central gyrus. Post-hoc tests, conducted after concatenating values across positions for this group, confirmed significantly lower Mahalanobis distances in the pre-central gyrus compared to the post-central gyrus, suggesting more advanced maturation (paired *t*-test: $T = -4.388$, (dof = 134), Cohen $D = 0.528$, $p < 0.001$). Higher Mahalanobis distances were observed in the lateral clusters when values were concatenated across regions, suggesting less advanced maturation (LAT vs. INT: $T = 5.933$ (dof = 89), Cohen $D = 0.770$, $p < 0.001$; LAT vs. MED: $T = 4.712$ (dof = 89), Cohen $D = 0.770$, $p < 0.001$), with no significant differences between INT and MED positions ($T = 0.380$ (dof = 89), Cohen $D = 0.125$, $p = 0.705$) (results FDR-corrected across the 3 comparisons).

In the PT_{TEA} group, assessing the Mahalanobis distances provides insight into the heterogeneous effects of prematurity on microstructural development across the clusters at term equivalent age. Although the distances were substantially lower than those observed in the PT_{Birth} group (Fig. 3a), suggesting that microstructural maturation continued *ex utero* and began to converge toward the profile of full-term (FT) infants, all regions and positions exhibited Mahalanobis distances significantly different from zero (Supplementary Table 3). ANCOVA modelling over this group highlighted a significant main effect of region, indicating that prematurity differentially affected the sensory and motor regions, but no main effect of position (Table 2). Although the patterns for the effect of region were less easy to discern visually in the PT_{TEA} group than in the PT_{Birth} group, post-hoc test confirmed lower distances in the pre- vs post-central gyrus when concatenating positions (paired *t*-test: $T = -4.169$ (dof = 176), Cohen $D = 0.332$, $p < 0.001$), in a similar way as close to birth. Consistently with the non-significant position effect, post-hoc tests on Mahalanobis distances between positions, after concatenating across regions, did not show significant differences (LAT vs. INT: $T = 0.604$ (dof = 117), Cohen $D = 0.112$, $p = 0.801$; LAT vs. MED: $T = 0.742$ (dof = 117), Cohen $D = 0.134$, $p = 0.801$; INT and MED positions ($T = 0.253$ (dof = 117), Cohen $D = 0.105$, $p = 0.801$, *p*-values FDR-corrected over 3 comparisons). The ANCOVA in the PT_{TEA} group also showed a significant effect of GA at birth, that we investigated further using linear regression. Although visually weak negative slopes were observed across all clusters, suggesting that higher GA at birth is associated with microstructure closer to full-term norms at TEA, this relationship reached statistical significance ($\alpha = 0.05$) only for the lateral post-central cluster (Post_{LAT}) but trends for Post_{INT} and Pre_{LAT} (Fig. 3b).

Table 2

For each PT group, ANCOVA analysis examining the relationship between Mahalanobis distance and GA at scan together with key factors: region (pre-/post-central gyri), and position and their interaction. The models account for hierarchical structure of the repeated measures across matched subjects, regions, and positions, with a nested error term. * $p < 0.05$; ** $p < 0.01$; *** $p < 0.001$.

	MH: PT _{Birth}			MH: PT _{TEA}		
	F	p	Partial η^2	F	p	Partial η^2
Covariates						
GA at birth	0.25 (1,43)	0.619	0.006	6.086 (1,57)	0.017*	0.096
Factors						
Region	25.48 (1,44)	< 0.001***	0.367	14.87 (1,58)	< 0.001***	0.204
Position	16.06 (2178)	< 0.001***	0.157	0.356 (2234)	0.701	0.003

4. Discussion

In this study of human infants, we parcellated the pre- and post-central gyri each into three cortical clusters along the lateral-ventral to medial-dorsal axis using diffusion MRI metrics. These clusters showed distinct microstructural profiles in both full-term neonates and preterm infants, including those scanned at TEA and close to birth, despite the effect of prematurity. Using a multivariate approach (Mahalanobis distance), we confirmed that preterm infants deviated from full-term reference at both time points, though deviations were smaller at TEA, consistent with ongoing maturation. Notably, the extent and pattern of deviations differed between the pre- and post-central gyri at both ages, suggesting differential effects of prematurity and maturation in motor versus sensory regions. Additionally, regional differences were also observed along the lateral-to-medial axis close to birth, supporting the hypothesis of asynchronous microstructural development across regions that become specialized for different body parts during the third trimester.

4.1. Parcellating cortical regions based on microstructural features

Cortical microstructure was assessed with a dedicated approach using advanced diffusion MRI and benefitting from the complementary information provided by DTI and NODDI models. Previous studies examining similar developmental windows have reported a systematic decrease in DTI diffusivity metrics with advancing cortical maturation (Ball et al., 2013; McKinstry et al., 2002; Ouyang et al., 2019b), supposed to reflect reduction in water content due to increasing cellular and organelle density. Correspondingly, one might expect an increase in NDI, although recent findings have been less consistent in this regard (Batalle et al., 2019) perhaps because cortical expansion counterbalances the neurite growth. Besides, the maturation-related increase in dendritic arbor complexity (Huttenlocher et al., 1987) and the decreasing radial organization of the cortex (Kostović et al., 2019) may account for observed decreases in DTI anisotropy and ODI reported during the preterm period.

Our findings align with these reported developmental trends related to cortical maturation. As expected, we observed the highest diffusivity and FA values, along with the lowest NDI and ODI, in preterms close to birth. These metrics showed intermediate values in preterms at TEA, and most mature profiles in full-term neonates. Among the two full-term groups, dMRI metrics were largely similar, except for ODI. This difference may reflect methodological factors, such as the potentially sub-optimal parametrization of the NODDI model for neonatal brain tissue or variable grey-white matter segmentation quality across subjects – particularly relevant given ODI's sensitivity to local tissue complexity like neurite orientation and dispersion that other metrics are less able to capture. Alternatively, group variability in GA at birth and/or PMA at scan and non-linear developmental changes around the perinatal period (Batalle et al., 2019) might have contributed to this ODI difference between the two full-term groups.

To further investigate regional microstructural variation within pre- and post-central gyri, we used an exploratory, data-driven clustering

approach on dMRI metrics from an independent group of full-term neonates, based on evidence that multimodal approaches improve the accuracy of microstructural evaluations compared to unimodal methods (Kulikova et al., 2015; Vaher et al., 2022). Although inter-metric correlations were not explicitly accounted for in our modelling, the spatial consistency of the resulting clusters supports the validity of the method. While direct vertex-wise clustering could have offered a more purely data-driven solution compared to the clustering of manually-delineated subdivisions, it might produce fragmented, spatially inconsistent regions. So we preferred a two-step method balancing anatomical plausibility with data-driven refinement. For simplicity and statistical power, left and right hemispheres were analysed together, which precluded assessment of inter-hemispheric asymmetries, current limitation that may be addressed in future studies.

Additionally, while the cortical clusters were defined based on full-term data, they showed consistent microstructural profiles in all groups (see below), suggesting they were relevant to compare preterm infants to full-term references. On the reverse, identifying clusters in each group independently would have impeded cross-group comparisons. Although including preterm infants in the clustering phase might have mitigated this issue, it was not possible due to limited availability of independent preterm data. Thus, a potential limitation of our approach is that regions defined on full-term brains may not perfectly correspond to preterm brain anatomy, differences in region size or position could cause some overlap with neighbouring areas and signal contamination. However, preterm signals, especially at birth, exhibit more extreme rather than blended values, suggesting that mapping inaccuracies are unlikely to drive the observed group differences. Moreover, the consistent microstructural profiles observed across all groups in diffusion metrics support the robustness of the cluster definitions and justify their use in comparative analyses.

4.2. Characterizing microstructural profiles of the pre- and post-central gyri

The pre- and post-central gyri of full-term neonates were parcellated along the lateral-to-medial axis into clusters showing distinct microstructural profiles (ANCOVA main effect of position). Systematic differences between the pre- and post-central gyri were further observed (ANCOVA main effect of region). These findings build on previous reports of distinct microstructural patterns in sensorimotor regions relative to other cortical areas (Batalle et al., 2019) and extend them by demonstrating that microstructural variations exist within sensorimotor regions as well. Additionally, similar microstructural differences have already been reported in adult brain, with studies showing particularly a higher orientation dispersion and myelination in the pre- compared to post-central gyrus, based on dMRI metrics (Fukutomi et al., 2018), and T1w/T2w ratio-derived myelination metric (Kuehn et al., 2017). This latter study also suggested that lateral positions of both pre- and post-central gyri (corresponding to the mouth representation in adults) have lower myelination than intermediate and medial positions at the mature stage. Furthermore, the adult myelin map showed a discontinuity that is consistent with the functional MRI (fMRI) activation map and the delimitation between functional contrasts for the face and the hand, and this discontinuity was more lateral and inferior in the post-central gyrus than in the pre-central gyrus (see Fig. 1 of (Kuehn et al., 2017)). Interestingly, the microstructural clusters that we identified in our study in neonates also demonstrated different spatial extent between the two gyri, the lateral cluster being more localized in lateral and inferior positions in the post- than in the pre-central gyrus.

Our findings suggest that such regional differences in microstructure might emerge early in cortical development. Despite variability in PMA at scan – and associated differences in brain size and gyrification – preterm neonates at both time points also showed consistent patterns of differences in diffusion metrics across both regions and along the lateral-to-medial axis. However, we refrained from directly interpreting these

spatial differences in terms of maturation due to the absence of normative, mature reference values for neonatal dMRI metrics. This would have required comparisons with adult datasets (Dubois et al., 2016), to enable the computation of maturational distances (Devischer et al., 2021; Kulikova et al., 2015). Yet, such comparisons would be methodologically challenging, given differences in brain size, cortical folding, and diffusion acquisition protocols across age groups.

Additionally, we remain cautious interpreting the potential functional significance of the identified clusters, as somatotopic mapping data were not available for the dHCP cohort. This limits our ability to interpret clusters in terms of specific body part representations. In adults, the lateral pre- and post-central regions typically correspond to facial areas, intermediate regions to the hands, and medial regions to the lower limbs. A visual comparison between our clusters and the only publicly available infant fMRI somatotopic maps (mouth, wrists, ankles; Dall'Orso et al., 2018) revealed neither a clear correspondence nor an outright mismatch. Thus, the relationship between early cortical microstructure and emerging functional specialization remains an open question.

4.3. Highlighting the effects of prematurity and maturation on sensorimotor regions

To better capture differences between infant groups, we adopted a multivariate approach based on Mahalanobis distances to compare preterm infants to a full-term reference, as proposed in previous study of sensorimotor white matter pathways in preterm infants at TEA (Neumane et al., 2022). Multivariate models, by leveraging inter-metric complementarity and typical individual variability, can more effectively capture complex, subtle group differences compared to univariate analyses. Here, we computed Mahalanobis distances using scaled dMRI metrics, with correction for PMA at scan and metric residuals over the whole cortex. Gestational age (GA) at birth was not included as a covariate, as it had minimal influence on individual metrics (data not shown) and was instead a variable of interest to evaluate whether GA influenced the prematurity distances. Sex was also not controlled for due to limited sample size, although it may contribute to inter-individual variability.

Using this approach, we found that preterm infants, both near birth and at term-equivalent age (TEA), significantly deviated from full-term profiles. These deviations were smaller at TEA, consistent with ongoing maturation. Our findings align with recent work showing region-specific cortical maturation trajectories (Ball et al., 2013; Batalle et al., 2019; Ouyang et al., 2019b), as well as heterogeneous regional effects of prematurity on cortical microstructure (Gondová et al., 2025; Ouyang et al., 2019). Our study extended these observations by providing a more fine-grained analysis within the sensorimotor cortex.

Close to birth, significant main effects of both region (pre- vs post-central gyrus) and position (lateral to medial) were found. The pre-central gyrus exhibited lesser impact of prematurity than the post-central gyrus, and lateral clusters appeared less impacted than intermediate and medial ones. Interestingly, medial clusters displayed divergent microstructural profiles across the pre- and post-central gyri compared to other positions, which may be attributed to unequal sizes of medial clusters, with Post_{MED} cluster spanning a relatively large portion of the cortex. At TEA, only the main effect of region (pre- vs post-central) remained significant, though the positional trend persisted within the pre-central gyrus.

Patterns across our results may be interpreted through two organizing principles. First, motor cortices appear to be more mature than sensory cortices during the preterm period and less affected by prematurity at TEA. This is consistent with our previous findings in white matter pathways, where motor connections were less vulnerable to prematurity than sensory pathways (Neumane et al., 2022). Second, cortical regions corresponding to the mouth showed more pronounced immaturity and greater sensitivity to prematurity than those associated

with the hands or lower limbs. This was somewhat unexpected given the early and intense functional use of the mouth in fetuses and neonates (e.g., intense suckling perceptions and experiences). Traditional developmental models suggest functional progression from top to bottom, and from medial to distal regions; however, our cortical findings align more closely with established neurodevelopmental gradients—particularly a caudal-to-rostral, and possibly medial-to-lateral pattern (Dubois et al., 2014; Yakovlev and Lecours, 1967).

Moreover, in approximately half of the cortical clusters, the Mahalanobis distance between preterm infants at TEA and full-terms systematically decreased with increasing GA at birth. This finding highlights that the degree of prematurity (extreme, very, moderate, late) significantly influences cortical microstructure, even at term-equivalent age. Collectively, our results support the notion that regions maturing later are more susceptible to prematurity-related disruption, emphasizing that the timing of preterm birth relative to a region's developmental trajectory is a critical determinant of its vulnerability.

5. Conclusion

Our findings demonstrate that the microstructural organization of the pre-central and post-central gyri is both region- and position-specific, emerges early in development, and is differentially influenced by prematurity. Notably, motor regions exhibited lesser impact of prematurity than somatosensory regions. The absence of neonatal functional data limits the interpretation of these results, particularly since structurally immature regions, such as the mouth area, are known to be functionally active early on, highlighting a potential dissociation between structural maturation and functional engagement. Future research, especially longitudinal studies integrating microstructure, function, and behaviour in preterm infants, will be essential to elucidate how these early structural differences relate to functional specialization and long-term neurodevelopmental outcomes.

CRedit authorship contribution statement

Alexandra Brandstaetter: Writing – review & editing, Writing – original draft, Methodology, Formal analysis, Data curation. **Andrea Gondova:** Writing – review & editing, Writing – original draft, Visualization, Validation, Methodology, Formal analysis. **Laurie Devisscher:** Writing – review & editing, Methodology. **Denis Riviere:** Writing – review & editing, Methodology. **Guillaume Auzias:** Writing – review & editing, Methodology. **Yann Leprince:** Writing – review & editing, Methodology. **Jessica Dubois:** Writing – review & editing, Writing – original draft, Validation, Supervision, Methodology, Funding acquisition, Conceptualization.

Funding

The developing Human Connectome Project was funded by the European Research Council under the European Union Seventh Framework Programme (FP/2007–2013)/ERC Grant Agreement no. 319456.

AG was supported by the CEA NUMERICS program. This project has received funding from the European Union's Horizon 2020 research and innovation programme under grant agreement No 800945 — NUMERICS — H2020-MSCA-COFUND-2017.

JD acknowledges funding support from the French government as part of the France 2030 programme (grant ANR-23-IAIU-0010, IHU Robert-Debré du Cerveau de l'Enfant), the French National Agency for Research (grant ANR-22-CE37-0028), the IdEx Université de Paris (ANR-18-IDEX-0001), the Fondation de France and Fondation Médicite (grants FdF-18-00092867 and FdF-20-00111908).

Declaration of Competing Interest

The authors declare that they have no known competing financial

interests or personal relationships that could have appeared to influence the work reported in this paper.

Acknowledgments

We thank Prof. Alard Roebroek of the Faculty for Psychology and Neuroscience at Maastricht University, who provided valuable support and guidance throughout the course of the Master's thesis project that forms the basis of this work.

Appendix A. Supporting information

Supplementary data associated with this article can be found in the online version at doi:10.1016/j.dcn.2025.101610.

Data availability

Data used in this study can be found here: <http://www.developingconnectome.org>.

References

- Adamson, C.L., Alexander, B., Ball, G., Beare, R., Cheong, J.L.Y., Spittle, A.J., Doyle, L.W., Anderson, P.J., Seal, M.L., Thompson, D.K., 2020. Parcellation of the neonatal cortex using Surface-based Melbourne Children's regional infant brain atlases (M-CRIB-S). *Sci. Rep.* 10 (1), 1–11. <https://doi.org/10.1038/s41598-020-61326-2>.
- Allievi, A.G., Arichi, T., Tusor, N., Kimpton, J., Arulkumaran, S., Counsell, S.J., Edwards, A.D., Burdet, E., 2016. Maturation of Sensori-Motor functional responses in the preterm brain. *Cereb. Cortex* 26 (1), 402–413. <https://doi.org/10.1093/cercor/bhv203>.
- Anderson, J., 1986. Sensory intervention with the preterm infant in the neonatal intensive care unit. *Am. J. Occup. Ther.* 40 (1), 19–26. <https://doi.org/10.5014/ajot.40.1.19>.
- Auzias, G., Lefevre, J., Le Troter, A., Fischer, C., Perrot, M., Regis, J., Coulon, O., 2013. Model-Driven harmonic parameterization of the cortical surface: HIP-HOP. *IEEE Trans. Med. Imaging* 32 (5), 873–887. <https://doi.org/10.1109/TMI.2013.2241651>.
- Ball, G., Srinivasan, L., Aljabar, P., Counsell, S.J., Durighel, G., Hajnal, J.V., Rutherford, M.A., Edwards, A.D., 2013. Development of cortical microstructure in the preterm human brain. *Proc. Natl. Acad. Sci.* 110 (23), 9541–9546. <https://doi.org/10.1073/pnas.1301652110>.
- Batalle, D., O'Muircheartaigh, J., Makropoulos, A., Kelly, C.J., Dimitrova, R., Hughes, E.J., Hajnal, J.V., Zhang, H., Alexander, D.C., Edwards, A.D., Counsell, S.J., 2019. Different patterns of cortical maturation before and after 38 weeks gestational age demonstrated by diffusion MRI in vivo. *NeuroImage* 185, 764–775. <https://doi.org/10.1016/j.neuroimage.2018.05.046>.
- Bozek, J., Makropoulos, A., Schuh, A., Fitzgibbon, S., Wright, R., Glasser, M.F., Coalson, T.S., O'Muircheartaigh, J., Hutter, J., Price, A.N., Cordero-Grande, L., Teixeira, R.P.A.G., Hughes, E., Tusor, N., Baruteau, K.P., Rutherford, M.A., Edwards, A.D., Hajnal, J.V., Smith, S.M., Robinson, E.C., 2018. Construction of a neonatal cortical surface Atlas using multimodal surface matching in the developing human connectome project. *NeuroImage* 179, 11–29. <https://doi.org/10.1016/j.neuroimage.2018.06.018>.
- Chauvel, M., Rheault, F., Rolland, C., Aubrain, K., Leroy, F., de Vareilles, H., Girard, G., Rivière, D., Hertz-Pannier, L., Mangin, J.F., Descoteaux, M., Dubois, J., 2020. Exploring the microstructural properties of the newborn sensorimotor network with diffusion MRI. *OHBM* 2020.
- Christiaens, D., Cordero-Grande, L., Pietsch, M., Hutter, J., Price, A.N., Hughes, E.J., Vecchiato, K., Deprez, M., Edwards, A.D., Hajnal, J.V., Tournier, J.-D., 2021. Scattered slice SHARD reconstruction for motion correction in multi-shell diffusion MRI. *NeuroImage* 225, 117437. <https://doi.org/10.1016/j.neuroimage.2020.117437>.
- Cong, X., Wu, J., Vittner, D., Xu, W., Hussain, N., Galvin, S., Fitzsimons, M., McGrath, J.M., Henderson, W.A., 2017. The impact of cumulative pain/stress on neurobehavioral development of preterm infants in the NICU. *Early Hum. Dev.* 108, 9–16. <https://doi.org/10.1016/j.earlhumdev.2017.03.003>.
- Cordero-Grande, L., Christiaens, D., Hutter, J., Price, A.N., Hajnal, J.V., 2019. Complex diffusion-weighted image estimation via matrix recovery under general noise models. *NeuroImage* 200, 391–404. <https://doi.org/10.1016/j.neuroimage.2019.06.039>.
- Cykowski, M.D., Coulon, O., Kochunov, P.V., Amunts, K., Lancaster, J.L., Laird, A.R., Glahn, D.C., Fox, P.T., 2008. The central sulcus: an Observer-Independent characterization of sulcal landmarks and depth asymmetry. *Cereb. Cortex* 18 (9), 1999–2009. <https://doi.org/10.1093/cercor/bhm224>.
- Dall'Orso, S., Arichi, T., Fitzgibbon, S.P., Edwards, A.D., Burdet, E., Muceli, S., 2022. Development of functional organization within the sensorimotor network across the perinatal period. *Hum. Brain Mapp.* 43 (7), 2249–2261. <https://doi.org/10.1002/hbm.25785>.

- Dall'Orso, S., Steinweg, J., Allievi, A.G., Edwards, A.D., Burdet, E., Arichi, T., 2018. Somatotopic mapping of the developing sensorimotor cortex in the preterm human brain. *Cereb. Cortex* 28 (7), 2507–2515. <https://doi.org/10.1093/cercor/bhy050>.
- Devisscher, L., Chauvel, M., Rolland, C., Labra, N., Aubrain, K., Leroy, F., de Vercelles, H., Hertz-Pannier, L., Grigis, A., Mangin, J.F., Dubois, J., 2021. Disentangling the differential maturation of sensorimotor cortices in newborns compared to adults. *OHBM* 2021.
- Dornier, A., Gérard, A., Leprince, Y., Hertz-Pannier, L., Mangin, J.-F., Barbu-Roth, M., Dubois, J., & Muret, D., 2025. On the typical development of the central sulcus in infancy: a longitudinal evaluation of its morphology and link to behaviour. <https://doi.org/10.1101/2025.02.19.639011>.
- Dubois, J., Alison, M., Counsell, S.J., Hertz-Pannier, L., Hüppi, P.S., Benders, M.J.N.L., 2021. MRI of the neonatal brain: a review of methodological challenges and neuroscientific advances. *J. Magn. Reson. Imaging* 53 (5), 1318–1343. <https://doi.org/10.1002/jmri.27192>.
- Dubois, J., Dehaene-Lambertz, G., Kulikova, S., Poupon, C., Hüppi, P.S., Hertz-Pannier, L., 2014. The early development of brain White matter: a review of imaging studies in fetuses, newborns and infants. *Neuroscience* 276, 48–71. <https://doi.org/10.1016/j.neuroscience.2013.12.044>.
- Dubois, J., Poupon, C., Thirion, B., Simonnet, H., Kulikova, S., Leroy, F., Hertz-Pannier, L., Dehaene-Lambertz, G., 2016. Exploring the early organization and maturation of linguistic pathways in the human infant brain. *Cereb. Cortex* 26 (5), 2283–2298. <https://doi.org/10.1093/cercor/bhv082>.
- Edwards, A.D., Rueckert, D., Smith, S.M., Abo Seada, S., Alansary, A., Almalbis, J., Allsop, J., Andersson, J., Arichi, T., Arulkumaran, S., Bastiani, M., Bataille, D., Baxter, L., Bozek, J., Braithwaite, E., Brandon, J., Carney, O., Chew, A., Christiaens, D., Hajnal, J.V., 2022. The developing human connectome project neonatal data release. *Front. Neurosci.* 16. <https://doi.org/10.3389/fnins.2022.886772>.
- Eyre, M., Fitzgibbon, S.P., Ciarrusta, J., Cordero-Grande, L., Price, A.N., Poppe, T., Schuh, A., Hughes, E., O'Keefe, C., Brandon, J., Cromb, D., Vecchiato, K., Andersson, J., Duff, E.P., Counsell, S.J., Smith, S.M., Rueckert, D., Hajnal, J.V., Arichi, T., Edwards, A.D., 2021. The developing human connectome project: typical and disrupted perinatal functional connectivity. *Brain* 144 (7), 2199–2213. <https://doi.org/10.1093/brain/awab118>.
- Fagard, J., Esseily, R., Jacquey, L., O'Regan, K., Somogyi, E., 2018. Fetal origin of sensorimotor behavior. *Front. Neurobotics* 12. <https://doi.org/10.3389/fnbot.2018.00023>.
- Flacking, R., Lehtonen, L., Thomson, G., Axelin, A., Ahlqvist, S., Moran, V.H., Ewald, U., Dykes, F., 2012. Closeness and separation in neonatal intensive care. *Acta Paediatr.* 101 (10), 1032–1037. <https://doi.org/10.1111/j.1651-2227.2012.02787.x>.
- Fukutomi, H., Glasser, M.F., Zhang, H., Autio, J.A., Coalson, T.S., Okada, T., Togashi, K., Van Essen, D.C., Hayashi, T., 2018. Neurite imaging reveals microstructural variations in human cerebral cortical gray matter. *NeuroImage* 182, 488–499. <https://doi.org/10.1016/j.neuroimage.2018.02.017>.
- Fyfe, K.L., Yiallourou, S.R., Wong, F.Y., Horne, R.S.C., 2014. The development of cardiovascular and cerebral vascular control in preterm infants. *Sleep. Med. Rev.* 18 (4), 299–310. <https://doi.org/10.1016/j.smrv.2013.06.002>.
- Germann, J., Chakravarty, M.M., Collins, D.L., Petrides, M., 2020. Tight coupling between morphological features of the central sulcus and somatomotor body representations: a combined anatomical and functional MRI study. *Cereb. Cortex* 30 (3), 1843–1854. <https://doi.org/10.1093/cercor/bhz208>.
- Gondová, A., Neumane, S., Arichi, T., Dubois, J., 2025. Early development and co-evolution of microstructural and functional brain connectomes: a multi-modal MRI study in preterm and Full-Term infants. *Hum. Brain Mapp.* 46 (5). <https://doi.org/10.1002/hbm.70186>.
- Gondová, A., Neumane, S., Leprince, Y., Mangin, J.-F., Arichi, T., Dubois, J., 2023. Predicting neurodevelopmental outcomes from neonatal cortical microstructure: a conceptual replication study. *NeuroImage Rep.* 3 (2), 100170. <https://doi.org/10.1016/j.ynirp.2023.100170>.
- Hernandez-Fernandez, M., Reguly, I., Jbabdi, S., Giles, M., Smith, S., Sotiropoulos, S.N., 2019. Using GPUs to accelerate computational diffusion MRI: from microstructure estimation to tractography and connectomes. *NeuroImage* 188, 598–615. <https://doi.org/10.1016/j.neuroimage.2018.12.015>.
- Hughes, E.J., Winchman, T., Padormo, F., Teixeira, R., Wurie, J., Sharma, M., Fox, M., Hutter, J., Cordero-Grande, L., Price, A.N., Allsop, J., Bueno-Conde, J., Tumor, N., Arichi, T., Edwards, A.D., Rutherford, M.A., Counsell, S.J., Hajnal, J.V., 2017. A dedicated neonatal brain imaging system. *Magn. Reson. Med.* 78 (2), 794–804. <https://doi.org/10.1002/mrm.26462>.
- Huttenlocher, P.R., de C.C., de Courten, C., 1987. The development of synapses in striate cortex of man. *Hum. Neurobiol.* 6 (1), 1–9.
- Hutter, J., Tournier, J.D., Price, A.N., Cordero-Grande, L., Hughes, E.J., Malik, S., Steinweg, J., Bastiani, M., Sotiropoulos, S.N., Jbabdi, S., Andersson, J., Edwards, A. D., Hajnal, J.V., 2018. Time-efficient and flexible design of optimized multishell HARDI diffusion. *Magn. Reson. Med.* 79 (3), 1276–1292. <https://doi.org/10.1002/mrm.26765>.
- Kostović, I., Sedmak, G., Judaš, M., 2019. Neural histology and neurogenesis of the human fetal and infant brain. *NeuroImage* 188, 743–773. <https://doi.org/10.1016/j.neuroimage.2018.12.043>.
- Kuehn, E., Dinse, J., Jakobsen, E., Long, X., Schäfer, A., Bazin, P.-L., Villringer, A., Sereno, M.I., Margulies, D.S., 2017. Body topography parcellates human sensory and motor cortex. *Cereb. Cortex* 27 (7), 3790–3805. <https://doi.org/10.1093/cercor/bhx026>.
- Kulikova, S., Hertz-Pannier, L., Dehaene-Lambertz, G., Buzmakov, A., Poupon, C., Dubois, J., 2015. Multi-parametric evaluation of the White matter maturation. *Brain Struct. Funct.* 220 (6), 3657–3672. <https://doi.org/10.1007/s00429-014-0881-y>.
- Lebenberg, J., Mangin, J.-F., Thirion, B., Poupon, C., Hertz-Pannier, L., Leroy, F., Adibpour, P., Dehaene-Lambertz, G., Dubois, J., 2019. Mapping the asynchrony of cortical maturation in the infant brain: a MRI multi-parametric clustering approach. *NeuroImage* 185, 641–653. <https://doi.org/10.1016/j.neuroimage.2018.07.022>.
- Makropoulos, A., Gousias, I.S., Ledig, C., Aljabar, P., Serag, A., Hajnal, J.V., Edwards, A. D., Counsell, S.J., Rueckert, D., 2014. Automatic whole brain MRI segmentation of the developing neonatal brain. *IEEE Trans. Med. Imaging* 33 (9), 1818–1831. <https://doi.org/10.1109/TMI.2014.2322280>.
- Makropoulos, A., Robinson, E.C., Schuh, A., Wright, R., Fitzgibbon, S., Bozek, J., Counsell, S.J., Steinweg, J., Vecchiato, K., Passerat-Palmbach, J., Lenz, G., Mortari, F., Tenev, T., Duff, E.P., Bastiani, M., Cordero-Grande, L., Hughes, E., Tumor, N., Tournier, J.D., Rueckert, D., 2018. The developing human connectome project: a minimal processing pipeline for neonatal cortical surface reconstruction. *NeuroImage* 173 (April 2017), 88–112. <https://doi.org/10.1016/j.neuroimage.2018.01.054>.
- Marshall, P.J., Meltzoff, A.N., 2015. Body maps in the infant brain. *Trends Cogn. Sci.* 19 (9), 499–505. <https://doi.org/10.1016/j.tics.2015.06.012>.
- Martin, J., Hamilton, B., & Osterman, M. 2023. Births in the United States, 2022. <https://doi.org/10.15620/cdc:131354>.
- McKinstry, R.C., Mathur, A.M., Miller, J.H., Ozcan, A., Snyder, A.Z., Schefft, G., Almlí, C. R., Shiran, S.I., Conturo, T.E., Neil, J.J., 2002. Radial organization of developing preterm human cerebral cortex revealed by Non-invasive water diffusion anisotropy MRI. *Cereb. Cortex* 12 (12), 1237–1243. <https://doi.org/10.1093/cercor/12.12.1237>.
- Neumane, S., Gondova, A., Leprince, Y., Hertz-Pannier, L., Arichi, T., Dubois, J., 2022. Early structural connectivity within the sensorimotor network: deviations related to prematurity and association to neurodevelopmental outcome. *Front. Neurosci.* 16. <https://doi.org/10.3389/fnins.2022.932386>.
- Ouyang, M., Dubois, J., Yu, Q., Mukherjee, P., Huang, H., 2019a. Delineation of early brain development from fetuses to infants with diffusion MRI and beyond. *NeuroImage* 185 (April), 836–850. <https://doi.org/10.1016/j.neuroimage.2018.04.017>.
- Ouyang, M., Dubois, J., Yu, Q., Mukherjee, P., Huang, H., 2019b. Delineation of early brain development from fetuses to infants with diffusion MRI and beyond. *NeuroImage* 185, 836–850. <https://doi.org/10.1016/j.neuroimage.2018.04.017>.
- Ouyang, M., Jeon, T., Sotiras, A., Peng, Q., Mishra, V., Halovanic, C., Chen, M., Chalak, L., Rollins, N., Roberts, T.P.L., Davatzikos, C., Huang, H., 2019. Differential cortical microstructural maturation in the preterm human brain with diffusion kurtosis and tensor imaging. *Proc. Natl. Acad. Sci.* 116 (10), 4681–4688. <https://doi.org/10.1073/pnas.1812156116>.
- Penfield, W., Boldrey, E., 1937. Somatic motor and sensory representation in the cerebral cortex of man as studied by electrical stimulation. *Brain* 60 (4), 389–443. <https://doi.org/10.1093/brain/60.4.389>.
- Rivière, D., Geffroy, D., Denghien, I., Souedet, N., Cointepas, Y., 2009. BrainVISA: an extensible software environment for sharing multimodal neuroimaging data and processing tools. *NeuroImage* 47, S163. [https://doi.org/10.1016/S1053-8119\(09\)71720-3](https://doi.org/10.1016/S1053-8119(09)71720-3).
- Teune, M.J., Bakhuizen, S., Gyamfi Bannerman, C., Opmeer, B.C., van Kaam, A.H., van Wassenaer, A.G., Morris, J.M., Mol, B.W.J., 2011. A systematic review of severe morbidity in infants born late preterm. *Am. J. Obstet. Gynecol.* 205 (4), 374.e1–374.e9. <https://doi.org/10.1016/j.ajog.2011.07.015>.
- Vaher, K., Galdi, P., Blesa Cabeza, M., Sullivan, G., Stoye, D.Q., Quigley, A.J., Thrippleton, M.J., Bogaert, D., Bastin, M.E., Cox, S.R., Boardman, J.P., 2022. General factors of White matter microstructure from DTI and NODDI in the developing brain. *NeuroImage* 254, 119169. <https://doi.org/10.1016/j.neuroimage.2022.119169>.
- de Vries, J.L.P., Visser, G.H.A., Prechtl, H.F.R., 1982. The emergence of fetal behaviour. I. qualitative aspects. *Early Hum. Dev.* 7 (4), 301–322. [https://doi.org/10.1016/0378-3782\(82\)90033-0](https://doi.org/10.1016/0378-3782(82)90033-0).
- Yakovlev, P.I., Lecours, A., 1967. The myelogenetic cycles of regional maturation of the brain. In: Minkowski, A. (Ed.), *Regional Development of the Brain in Early Life*. Blackwell.
- Yamada, Y., Kanazawa, H., Iwasaki, S., Tsukahara, Y., Iwata, O., Yamada, S., Kuniyoshi, Y., 2016. An embodied brain model of the human foetus. *Sci. Rep.* 6 (1), 27893. <https://doi.org/10.1038/srep27893>.
- Zhang, H., Schneider, T., Wheeler-Kingshott, C.A., Alexander, D.C., 2012. NODDI: practical in vivo neurite orientation dispersion and density imaging of the human brain. *NeuroImage* 61 (4), 1000–1016. <https://doi.org/10.1016/j.neuroimage.2012.03.072>.